Nuclear Instruments and Methods in Physics Research A 787 (2015) 344–347

Contents lists available at ScienceDirect

Nuclear Instruments and Methods in Physics Research A

journal homepage: www.elsevier.com/locate/nima

G4SiPM: A novel silicon photomultiplier simulation package for Geant4

Tim Niggemann *, Erik Dietz-Laursonn, Thomas Hebbeker, Andreas Künsken, Markus Lauscher, Markus Merschmeyer

III. Physikalisches Institut, RWTH Aachen University, Germany

ARTICLE INFO

Available online 24 January 2015

Keywords:
Afterpulsing
Dynamic range
Geant4
Optical crosstalk
Silicon photomultipliers
Thermal noise

ABSTRACT

The signal of silicon photomultipliers (SiPMs) depends not only on the number of incoming photons but also on thermal and correlated noise of which the latter is difficult to handle. Additionally, the properties of SiPMs vary with the supplied bias voltage and the ambient temperature.

The purpose of the G4SiPM simulation package is the integration of a detailed SiPM simulation into Geant4 which is widely used in particle physics. The prediction of the G4SiPM simulation code is validated with a laboratory measurement of the dynamic range of a $3 \times 3\ \mathrm{mm}^2$ SiPM with 3600 cells manufactured by Hamamatsu.

1. Introduction

Silicon photomultipliers (SiPMs) are pixelated photon detectors for the detection of light on a single-photon basis [1]. They have a high photon detection efficiency (PDE) of typically 40%. Prototype devices demonstrate a PDE of over 60% and thus render them a promising candidate for future experiments [2]. SiPMs are subject to noise: the unavoidable thermal noise, as well as optical crosstalk, which can trigger different regions of the SiPM in coincidence, and furthermore after-pulses which are delayed additional triggers in the same cell created by the release of trapped electrons [1]. Thus, it is not trivial to predict the exact response of the SiPM when exposed to light [3].

For this purpose, the Monte-Carlo simulation G4SiPM has been developed which integrates into Geant4 which is a toolkit widely used in particle physics in detector simulations [4]. The input variables for the simulation are phenomenological quantities which can either be determined in the laboratory or be taken from existing publications (e.g. [5–7]). The triggering of the SiPM is simulated on a single-cell level to model the recovery behavior and also the creation of correlated noise.

To cross-check the prediction of the G4SiPM simulation, dynamic range measurements of several SiPM devices [8,9] have been performed in collaboration with the UGR Granada.[1] The number of triggered SiPM cells has been measured as a function of the number of incoming photons per light pulse.

2. SiPM model

SiPMs consist of single cells, i.e. Geiger-mode avalanche photodiodes (G-APDs), connected in parallel through a resistor R_q. Incoming photons, which are absorbed in a G-APD, create an electron–hole pair which in turn triggers an avalanche. The avalanche is blocked by the quenching resistor R_q in series to the diode [10].

Many properties of the SiPM depend on the over-voltage V_{ov}, i.e. the excess of the bias-voltage V_{bias} over the breakdown-voltage V_{break} of the G-APDs:

$$V_{\mathrm{ov}}(T) = V_{\mathrm{bias}} - V_{\mathrm{break}}(T) \tag{1}$$

whereby the breakdown-voltage itself depends approximately linearly on the temperature in a small temperature range (e.g. from 0 °C to 50 °C)

$$V_{\mathrm{break}}(T) = V_0(T_0) + \beta(T - T_0) \tag{2}$$

with e.g. $\beta \approx 50\ \mathrm{mV\ K^{-1}}$ for Hamamatsu devices [11]. The dependency of the SiPM on V_{ov} and T is included in G4SiPM. Furthermore, the properties of the SiPM can be interpolated for a setting of V_{break} and T which has not been supplied by the user.

2.1. Phenomenological model

The square cells on a SiPM are separated for electrical isolation and wiring purposes [1]. Thus only the fraction $\epsilon_{\mathrm{geom}} < 1$, also referred to as geometrical fill factor, of the SiPM surface is sensitive to incoming light.

* Corresponding author.
E-mail address: niggemann@physik.rwth-aachen.de (T. Niggemann).
URL: http://www.forge.physik.rwth-aachen.de/projects/g4sipm (T. Niggemann).

[1] Paper in preparation.

http://dx.doi.org/10.1016/j.nima.2015.01.067
0168-9002/

The photon detection efficiency (PDE) is one of the most important properties of photon counting devices such as SiPMs. It is defined by

$$\mathrm{PDE}(\lambda) = \epsilon_{\mathrm{geom}}\epsilon_{\mathrm{trig}}\ \mathrm{QE}(\lambda) \tag{3}$$

with the geometrical fill factor ϵ_{geom} as described above, the trigger probability ϵ_{trig}, which is the probability for the primary electron–hole pair to create an avalanche, and the quantum efficiency $\mathrm{QE}(\lambda)$, which is the probability to create the primary electron–hole pair, as a function of the photon wavelength λ [12].

Additionally the PDE is reduced for photons impinging at non-normal angles due to multilayer Fresnel reflections at the coating and the silicon chip [13,14].

When a photon hits the SiPM silicon in G4SiPM, initially it is checked whether the photon hits a cell, secondly the photon is accepted as detected with a probability of

$$P = \frac{\mathrm{PDE}(\lambda)}{\epsilon_{\mathrm{geom}}T(\theta)} \tag{4}$$

with the Fresnel transmission efficiency $T(\theta)$ for two optical boundaries (entrance window and silicon) as a function of the angle of incidence of the photon on the entrance window.

Even if operated in the dark, SiPM cells can break down accidentally due to thermal and secondary correlated noise effects [1].

Dark noise in G4SiPM is simulated after completion of the photon tracking.

To simulate the SiPM with dark noise on a single cell basis, a chronologically sorted trigger queue is created (c.f. Fig. 1). Each cell-trigger from the photon tracking gets sorted into the queue along with the creation process name ("photon", "thermal", "crosstalk" or "afterpulse"), a cell identifier and the exact point in time.

Subsequently, triggers from thermal noise are added to the queue.

Thermally excited electrons in the silicon lattice may have enough kinetic energy to create the initial pair of charge carriers which initiate a breakdown [1]. A typical rate for various current devices is $f_{\mathrm{th}} \approx 100\ \mathrm{kHz\ mm^{-2}}$ at $V_{\mathrm{ov}} = \mathbb{O}(1\ \mathrm{V})$ and room temperature.

Thermal noise is added to the trigger queue in a time window considerably larger than the time window in which the photons have been simulated to allow the Monte-Carlo model to reach a steady-like state.

From now on, the G4SiPM trigger queue is traversed. For each trigger, regardless of its origin, correlated noise, as described in the following, is computed.

Due to charge carrier recombination, roughly one photon per 10^5 generated electron–hole pairs is emitted during a breakdown with wavelengths $< 1\ \mu\mathrm{m}$ [15]. The photon can travel through the silicon to a neighboring pixel and cause a coincident cell breakdown. The probability for one trigger to invoke exactly one additional trigger due to crosstalk is $P_{\mathrm{ct}} = \mathbb{O}(10\%)$ for Hamamatsu devices at $V_{\mathrm{ov}} = \mathbb{O}(1\ \mathrm{V})$ [6].

For the prompt optical crosstalk only the four nearest neighboring cells are considered in G4SiPM [16]. The number of crosstalk-triggers succeeding a single cell-trigger is picked from a binomial distribution

$$P(k) = \binom{n}{k} p^k (1-p)^{n-k} \tag{5}$$

with $n = 4$ trials and the probability

$$p = 1 - (1 - P_{\mathrm{ct}})^{1/n} \tag{6}$$

given $P(0) = 1 - P_{\mathrm{ct}}$.

During the avalanche, electrons can be trapped at impurities of the silicon [17]. They are released according to an exponential decay with either one of two characteristic time constants: the short $\tau_{\mathrm{ap,s}} = \mathbb{O}(10\ \mathrm{ns})$ and the long $\tau_{\mathrm{ap,l}} = \mathbb{O}(100\ \mathrm{ns})$. The probabilities for these two components are $P_{\mathrm{ap,s}}$ and $P_{\mathrm{ap,l}}$.

For each afterpulsing component separately, the number of afterpulsing triggers is picked from a Poisson distribution:

$$P(k) = \frac{\lambda^k}{k!} e^{-\lambda} \tag{7}$$

with the mean

$$\lambda = -\ln(1 - P_{\mathrm{ap}}) \tag{8}$$

given $P(0) = 1 - P_{\mathrm{ap}}$.

2.2. Electrical model

In principle, the G-APDs can be modeled as a capacitor with a capacitance of C_d (c.f. Fig. 2) [10]. The breakdown is a spontaneous discharge of the capacitance with the intrinsic G-APD resistance R_d connected in parallel. Measurements yield $C_d \approx 0.1\ \mathrm{pF}$ [18] and $R_d \approx 1\ \mathrm{k\Omega}$ [10] depending on the device structure.

In reality, G-APDs have a quenching resistance $R_q \approx 100\ \mathrm{k\Omega}$ connected in series to the G-APD which stops the self-sustaining avalanche in the silicon by limiting the current flow. The minimum current required for a self-sustaining avalanche is approximately $I_q = 20\ \mu\mathrm{A}$ [10]. Now, in the equivalent circuit, the capacitance C_d is fully drained and the voltage over the G-APD recharges according to

$$V_{\mathrm{gapd}}(t) = V_{\mathrm{ov}}\left(1 - e^{-t/\tau_{\mathrm{rec}}}\right) \tag{9}$$

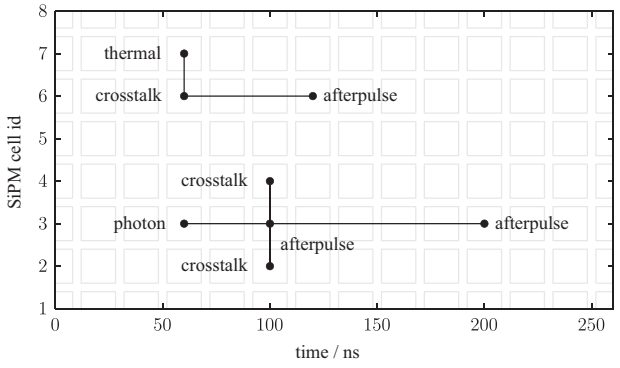

Fig. 1. Sketch of the chronologically sorted trigger queue implemented in G4SiPM. The recharge status of each cell determined by the time passed after the preceding cell-trigger. While traversing the queue, all triggers are handled in an equal manner and correlated noise triggers are added subsequently.

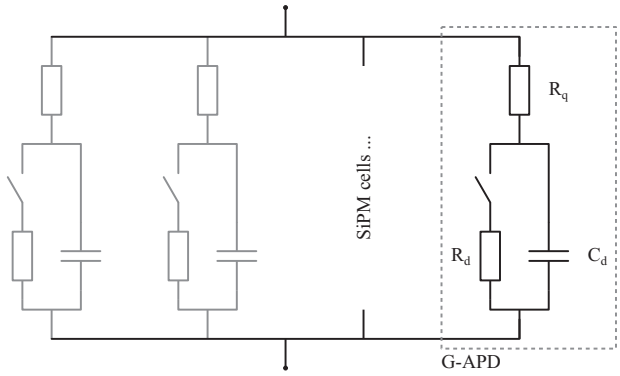

Fig. 2. Equivalent circuit of the G-APDs in a SiPM. A G-APD can be modeled as a capacitor C_d with an intrinsic resistance R_d and a quenching resistor R_q connected in series. Adapted from [10].

with the characteristic recharge time constant $\tau_{\text{rec}} = C_d R_q = \mathbb{O}(10\text{ ns})$. The time needed to recover the voltage $V_q = I_q R_d + V_{\text{break}}$, at which the current of a subsequent breakdown exceeds I_q, can be derived:

$$t_{\text{dead}} = -\tau_{\text{rec}} \left(\ln\left(1 - \frac{V_q}{V_{\text{bias}}}\right) - \ln\left(1 - \frac{V_{\text{break}}}{V_{\text{bias}}}\right) \right) \tag{10}$$

which is the real dead time of SiPMs in the G4SiPM simulation and in the order of $t_{\text{dead}} \approx \mathbb{O}(100\text{ ps})$. It is assumed that the probability for an electron–hole pair to trigger an avalanche ϵ_{trig} is recovered within t_{dead}.

The gain G of a SiPM (typical value $G = 10^6$) is given by the number of electrons per avalanche since it represents the multiplication factor of the initial signal which is in this case one electron–hole pair [1]. In the equivalent circuit, the gain is proportional to the current charge of the cell capacitance C_d and thus proportional to $V_{\text{gapd}}(t)$ with the time duration t to the preceding breakdown [10].

The probabilities for correlated noise are proportional to the current over-voltage and are interpolated according to $P \propto V_{\text{gapd}}(t)^2$ under the assumption $P(V_{\text{break}} = 0) = 0$.

Additionally, the gain systematically varies over the SiPM surface [5] and from breakdown to breakdown by approximately 10% [19] which is also implemented in G4SiPM.

In summary, the following parameters are required by G4SiPM for a successful ray tracing: PDE(λ) and ϵ_{geom}. However, for the noise simulation, f_{th}, P_{ct}, $P_{\text{ap,s}}$, $P_{\text{ap,l}}$, $\tau_{\text{ap,s}}$, $\tau_{\text{ap,l}}$ and τ_{rec} are required. If desired, all parameters can be supplied as a function of V_{break} and T.

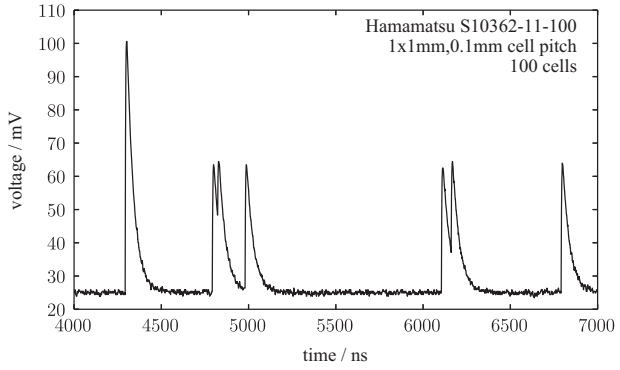

Fig. 3. G4SiPM simulation of a voltage trace of a SiPM as it can be measured e.g. with an oscilloscope.

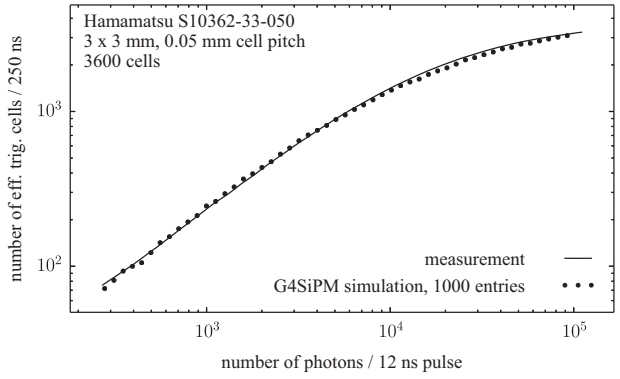

Fig. 4. The number of triggered SiPM cells as a function of incoming photons per light pulse (rectangular, 12 ns width) integrated in a 250 ns time window. The results of the G4SiPM simulation are denoted as dots, the measurement results as solid line. Both agree within 5%.

In terms of computing costs, 1 ms of SiPM dark noise (3600 cells) can be generated in less than 1 s (< 5 s including voltage trace, c.f. Fig. 3) with a memory usage of less than 350 MB (single 3 GHz CPU).

3. Comparison to a dynamic range measurement

To demonstrate the ability of the G4SiPM package to predict the response of the SiPM regardless of the incoming photon flux, a measurement of the dynamic range has been performed. The SiPM properties for G4SiPM have been taken from [5–7,18]. The light source was an LED with $\lambda = 485$ nm driven by a custom-made pulser. Primarily, the irradiation of the LED has been characterized using a calibrated PIN diode. Secondly, the pulsed LED is used to illuminate the SiPMs with light pulses of varying intensity and length. The SiPM is operated in a cooling box for temperature controlled measurements. The readout electronics consist of a readout circuit proposed by the manufacturer and a charge-to-digital-converter. Finally, the number of effectively triggered SiPM cells within a certain integration window was measured as a function of the number of photons per pulse.

As presented in Fig. 4, G4SiPM can successfully reproduce the dynamic range measurement of a Hamamatsu device for a certain LED pulse width and over-voltage within 5%.

4. Summary

The G4SiPM simulation package can be used to simulate SiPMs over their entire dynamic range. Comparisons of the simulation results to a dynamic range measurement of a Hamamatsu device yield very good agreement.

The simulation will be tested against multiple measurements performed with Hamamatsu and Ketek SiPMs at different over-voltages and LED pulse widths in the near future.

Acknowledgments

This work is funded by the European astroparticle physics network ASPERA and the German Federal Ministry of Education and Research BMBF under Contract no. 05A11PAA. The dynamic range measurements have been performed in collaboration with the Universidad de Granada, Departamento de Física Teórica y del Cosmos. Additionally, the authors would like to thank the mechanical and electronics workshops in Aachen and the CMS working group Aachen.

References

[1] D. Renker, E. Lorenz, Journal of Instrumentation 4 (04) (2009) P04004.
[2] B. Dolgoshein, et al., Nuclear Instruments and Methods in Physics Research Section A 695 (2012).
[3] H.T. van Dam, et al., IEEE Transactions on Nuclear Science NS-57 (4) (2010).
[4] S. Agostinelli, et al., Nuclear Instruments and Methods in Physics Research Section A 506 (3) (2003).
[5] P. Eckert, et al., Nuclear Instruments and Methods in Physics Research Section A 620 (2) (2010).
[6] M. Lauscher, Characterisation studies of silicon photomultipliers for the detection of fluorescence light from extensice air showers (Master's thesis), RWTH Aachen University (2012).
[7] T. Niggemann, et al., Status of the silicon photomultiplier telescope FAMOUS for the fluorescence detection of UHECRs, dep 3 (2013) d2N*γ*, *arXiv:1502.00792*.
[8] Hamamatsu Photonics, ⟨http://www.hamamatsu.com⟩.
[9] Ketek GmbH, ⟨http://www.ketek.net⟩.
[10] S. Cova, et al., Applied Optics 35 (12) (1996).
[11] W. Shen, Development of high performance readout ASICs for silicon photomultipliers (SiPMs) (Ph.D. thesis), 2012.
[12] C. Piemonte, Nuclear Instruments and Methods in Physics Research Section A 568 (1) (2006).
[13] D. Wilson, Angular dependence of the relative photon detection efficiency of silicon photomultipliers (Bachelor's thesis), 2012.

[14] P. Lecoq, et al., Sipm angular response and enhanced light extraction, in: NSS, 2013.
[15] R. Mirzoyan, R. Kosyra, H.G. Moser, Nuclear Instruments and Methods in Physics Research Section A 610 (1) (2009).
[16] L. Gallego, et al., Journal of Instrumentation 8 (05) (2013) P05010.
[17] Y. Du, F. Retiere, Nuclear Instruments and Methods in Physics Research Section A 596 (3) (2008).
[18] F. Scheuch, et al., Nuclear Instruments and Methods in Physics Research Section A (2014), http://dx.doi.org/10.1016/j.nima.2015.01.066, this issue.
[19] P. Buzhan, et al., ICFA Instrumentation Bulletin 21 (2001) 28.